



# Chapter 13

## LINEAR ANALYSIS OF SPLIT AND FACTORED FORMS

### 13.1 Introduction

In Section 4.5 we introduced the concept of the representative equation, and used it in Chapter 7 to study the stability, accuracy, and convergence properties of time-marching schemes. The question is: Can we find a similar equation that will allow us to evaluate the stability and convergence properties of split and factored schemes? The answer is yes — for certain forms of linear model equations.

The analysis in this chapter is useful for estimating the stability and steady-state properties of a wide variety of time-marching schemes that are variously referred to as time-split, fractional-step, hybrid, and (approximately) factored. When these methods are applied to practical problems, the results found from this analysis are neither necessary nor sufficient to guarantee stability. However, if the results indicate that a method has an instability, the method is probably not suitable for practical use.

### 13.2 The Representative Equation for Circulant Operators

Consider linear PDE's with coefficients that are fixed in both space and time and with boundary conditions that are periodic. We have seen that under these conditions a semi-discrete approach can lead to circulant matrix difference operators, and we discussed circulant eigensystems<sup>1</sup> in Section 4.4. In this and the following section

---

<sup>1</sup>See also the discussion on Fourier stability analysis in Section 7.7.

we assume circulant systems and our analysis *depends critically on the fact that all circulant matrices commute and have a common set of eigenvectors*.

Suppose, as a result of space differencing the PDE, we arrive at a set of ODE's that can be written

$$\frac{d\vec{u}}{dt} = A_{ap}\vec{u} + A_{bp}\vec{u} - \vec{f}(t) \quad (13.1)$$

where the subscript  $p$  denotes a circulant matrix. Since both matrices have the same set of eigenvectors, we can use the arguments made in Section 4.3.3 to uncouple the set and form the  $M$  set of independent equations

$$\begin{aligned} w'_1 &= (\lambda_a + \lambda_b)_1 w_1 - g_1(t) \\ &\vdots \\ w'_m &= (\lambda_a + \lambda_b)_m w_m - g_m(t) \\ &\vdots \\ w'_M &= (\lambda_a + \lambda_b)_M w_M - g_M(t) \end{aligned} \quad (13.2)$$

The analytic solution of the  $m$ 'th line is

$$w_m(t) = c_m e^{(\lambda_a + \lambda_b)_m t} + P.S.$$

Note that each  $\lambda_a$  pairs with one, and only one<sup>2</sup>,  $\lambda_b$  since they must share a common eigenvector. This suggests (see Section 4.5:

The representative equation for split, circulant systems is

$$\frac{du}{dt} = [\lambda_a + \lambda_b + \lambda_c + \dots]u + ae^{\mu t} \quad (13.3)$$

where  $\lambda_a + \lambda_b + \lambda_c + \dots$  are the sum of the eigenvalues in  $A_a$ ,  $A_b$ ,  $A_c$ ,  $\dots$  that share the same eigenvector.

## 13.3 Example Analysis of Circulant Systems

### 13.3.1 Stability Comparisons of Time-Split Methods

Consider as an example the linear convection-diffusion equation:

$$\frac{\partial u}{\partial t} + a \frac{\partial u}{\partial x} = \nu \frac{\partial^2 u}{\partial x^2} \quad (13.4)$$

<sup>2</sup>This is to be contrasted to the developments found later in the analysis of 2-D equations.

If the space differencing takes the form

$$\frac{d\vec{u}}{dt} = -\frac{a}{2\Delta x}B_p(-1, 0, 1)\vec{u} + \frac{\nu}{\Delta x^2}B_p(1, -2, 1)\vec{u} \quad (13.5)$$

the convection matrix operator and the diffusion matrix operator, can be represented by the eigenvalues  $\lambda_c$  and  $\lambda_d$ , respectively, where (see Section 4.4.2):

$$\begin{aligned} (\lambda_c)_m &= \frac{ia}{\Delta x} \sin \theta_m \\ (\lambda_d)_m &= -\frac{4\nu}{\Delta x^2} \sin^2 \frac{\theta_m}{2} \end{aligned} \quad (13.6)$$

In these equations  $\theta_m = 2m\pi/M$ ,  $m = 0, 1, \dots, M-1$ , so that  $0 \leq \theta_m \leq 2\pi$ . Using these values and the representative equation 13.4, we can analyze the stability of the two forms of simple time-splitting discussed in Section 12.2. In this section we refer to these as

1. the explicit-implicit Euler method, Eq. 12.10.
2. the explicit-explicit Euler method, Eq. 12.8.

### 1. The Explicit-Implicit Method

When applied to Eq. 13.4, the characteristic polynomial of this method is

$$P(E) = (1 - h\lambda_d)E - (1 + h\lambda_c)$$

This leads to the principal  $\sigma$  root

$$\sigma = \frac{1 + i\frac{ah}{\Delta x} \sin \theta_m}{1 + 4\frac{h\nu}{\Delta x^2} \sin^2 \frac{\theta_m}{2}}$$

where we have made use of Eq. 13.6 to quantify the eigenvalues. Now introduce the dimensionless numbers

$$\begin{aligned} C_n &= \frac{ah}{\Delta x} \quad , \quad \text{Courant number} \\ R_\Delta &= \frac{a\Delta x}{\nu} \quad , \quad \text{mesh Reynolds number} \end{aligned}$$

and we can write for the absolute value of  $\sigma$

$$|\sigma| = \frac{\sqrt{1 + C_n^2 \sin^2 \theta_m}}{1 + 4\frac{C_n}{R_\Delta} \sin^2 \frac{\theta_m}{2}} \quad , \quad 0 \leq \theta_m \leq 2\pi \quad (13.7)$$

A simple numerical parametric study of Eq. 13.7 shows that the critical range of  $\theta_m$  for any combination of  $C_n$  and  $R_\Delta$  occurs when  $\theta_m$  is near 0 (or  $2\pi$ ). From this we find that the condition on  $C_n$  and  $R_\Delta$  that make  $|\sigma| \approx 1$  is

$$\left[1 + C_n^2 \sin^2 \epsilon\right] = \left[1 + 4 \frac{C_n}{R_\Delta} \sin^2 \frac{\epsilon}{2}\right]^2$$

As  $\epsilon \rightarrow 0$  this gives the stability region

$$C_n < \frac{2}{R_\Delta}$$

which is bounded by a hyperbola and shown in Fig. 13.1.

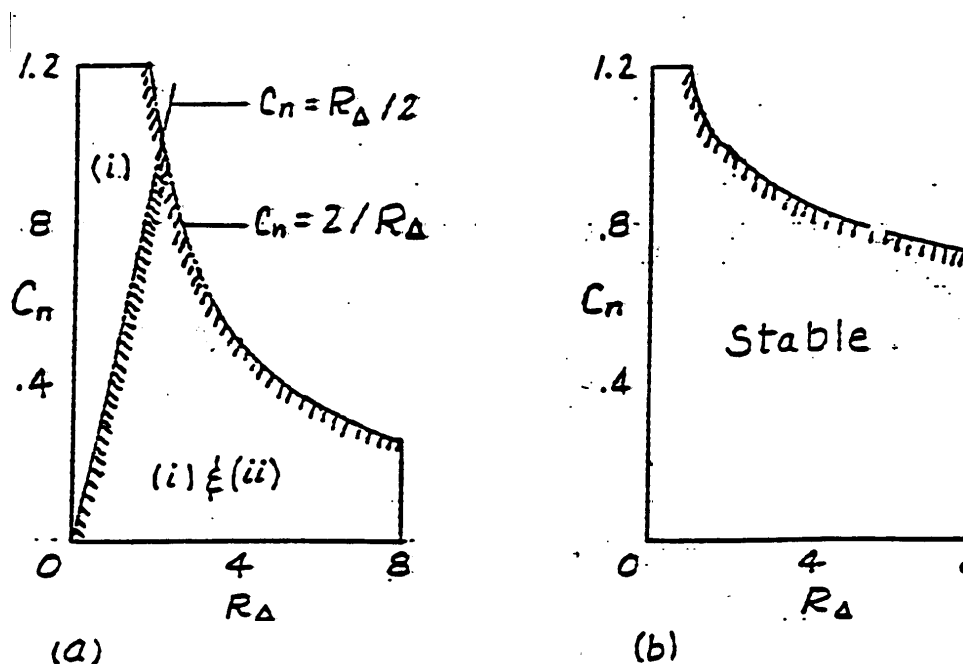


Figure 13.1: Stability Regions For Some Factored Methods.

## 2. The Explicit-Explicit Method

An analysis similar to the one given above shows that this method produces

$$|\sigma| = \sqrt{1 + C_n^2 \sin^2 \theta_m} \left[1 - 4 \frac{C_n}{R_\Delta} \sin^2 \frac{\theta_m}{2}\right] ; \quad 0 \leq \theta_m \leq 2\pi$$

Again a simple numerical parametric study shows that this has two critical ranges of  $\theta_m$ , one near 0, which yields the same result as in the previous example, and the other near  $180^\circ$ , which produces the constraint that

$$C_n < \frac{1}{2}R_\Delta \quad \text{for } R_\Delta \leq 2$$

This bound is also shown in Fig. 13.1 forming the straight line through the origin. The totally explicit, factored method has a much smaller region of stability when  $R_\Delta$  is small, as we should have expected.

### 13.3.2 Analysis of a Second-Order Time-Split Method

Next let us analyze a more practical method that has been used in serious computational analysis of turbulent flows. This method applies to a flow in which there is a combination of diffusion and periodic convection. The convection term is treated explicitly using the second-order Adams-Bashforth method. The diffusion term is integrated implicitly using the trapezoidal method. Our model equation is again the linear convection-diffusion equation 13.4 which we split in the fashion of Eq. 13.5. In order to evaluate the accuracy, as well as the stability, we include the forcing function in the representative equation and study the effect of our hybrid, time-marching method on the equation

$$u' = \lambda_c u + \lambda_d u + ae^{\mu t}$$

First let us find expressions for the two polynomials,  $P(E)$  and  $Q(E)$ . The characteristic polynomial follows from the application of the method to the homogeneous equation, thus

$$u_{n+1} = u_n + \frac{1}{2}h\lambda_c(3u_n - u_{n-1}) + \frac{1}{2}h\lambda_d(u_{n+1} + u_n)$$

This produces

$$P(E) = (1 - \frac{1}{2}h\lambda_d)E^2 - (1 + \frac{3}{2}h\lambda_c + \frac{1}{2}h\lambda_d)E + \frac{1}{2}h\lambda_c$$

The form of the particular polynomial depends upon whether the forcing function is carried by the AB2 method or by the trapezoidal method. In the former case it is

$$Q(E) = \frac{1}{2}h(3E - 1) \tag{13.8}$$

and in the latter

$$Q(E) = \frac{1}{2}h(E^2 + E) \tag{13.9}$$

**Accuracy**

From the characteristic polynomial we see that there are two  $\sigma$ -roots and they are given by the equation

$$\sigma = \frac{1 + \frac{3}{2}h\lambda_c + \frac{1}{2}h\lambda_d \pm \sqrt{\left(1 + \frac{3}{2}h\lambda_c + \frac{1}{2}h\lambda_d\right)^2 - 2h\lambda_c\left(1 - \frac{1}{2}h\lambda_d\right)}}{2\left(1 - \frac{1}{2}h\lambda_d\right)} \quad (13.10)$$

The principal  $\sigma$ -root follows from the plus sign and one can show

$$\sigma_1 = 1 + (\lambda_c + \lambda_d)h + \frac{1}{2}(\lambda_c + \lambda_d)^2 h^2 + \frac{1}{4}(\lambda_d^3 + \lambda_c \lambda_d^2 - \lambda_c^2 \lambda_d - \lambda_c^3) h^3$$

From this equation it is clear that  $\frac{1}{6}\lambda^3 = \frac{1}{6}(\lambda_c + \lambda_d)^3$  does not match the coefficient of  $h^3$  in  $\sigma_1$ , so

$$er_\lambda = O(h^3)$$

Using  $P(e^{\mu h})$  and  $Q(e^{\mu h})$  to evaluate  $er_\mu$  in Section 6.5.3, one can show

$$er_\mu = O(h^3)$$

using *either* Eq. 13.8 *or* Eq. 13.9. These results show that, for the model equation, the hybrid method retains the second-order accuracy of its individual components.

**Stability**

The stability of the method can be found from Eq. 13.10 by a parametric study of  $c_n$  and  $R_\Delta$  defined in Eq. 13.7. This was carried out in a manner similar to that used to construct Fig. 13.1a. The results are plotted in Fig. 13.1b. For values of  $R_\Delta \geq 2$  this second-order method has a much greater region of stability than the first-order explicit-implicit method given by Eq. 12.10 and shown in Fig. 13.1.

## 13.4 The Representative Equation for Space-Split 2-D Operators

Consider the 2-D model<sup>3</sup> equations

$$\frac{\partial u}{\partial t} = \frac{\partial^2 u}{\partial x^2} + \frac{\partial^2 u}{\partial y^2} \quad (13.11)$$

---

<sup>3</sup>The extension of the following to 3-D is simple and straightforward.

13.4. THE REPRESENTATIVE EQUATION FOR SPACE-SPLIT 2-D OPERATORS 215

and

$$\frac{\partial u}{\partial t} + a_x \frac{\partial u}{\partial x} + a_y \frac{\partial u}{\partial y} = 0 \quad (13.12)$$

Reduce either of these, by means of spatial differencing approximations, to the coupled set of ODE's:

$$\frac{dU}{dt} = [A_x + A_y]U + (bc)$$

for the space vector  $U$ . The form of the  $A_x$  and  $A_y$  matrices for three-point central differencing schemes are shown in Eqs. 12.22 and 12.23 for the  $3 \times 4$  mesh shown in Sketch 12.12. Let us inspect the structure of these matrices closely to see how we can diagonalize  $[A_x + A_y]$  in terms of the individual eigenvalues of the two matrices considered separately.

First we write these matrices in the form

$$A_x^{(x)} = \begin{bmatrix} B & & \\ & B & \\ & & B \end{bmatrix} \quad A_y^{(x)} = \begin{bmatrix} \tilde{b}_0 \cdot I & \tilde{b}_1 \cdot I & \\ \tilde{b}_{-1} \cdot I & \tilde{b}_0 \cdot I & \tilde{b}_1 \cdot I \\ & \tilde{b}_{-1} \cdot I & \tilde{b}_0 \cdot I \end{bmatrix}$$

where  $B$  is a banded matrix of the form  $B(b_{-1}, b_0, b_1)$ . Now find the block eigenvector matrix that diagonalizes  $B$  and use it to diagonalize  $A_x^{(x)}$ . Thus

$$\begin{bmatrix} X^{-1} & & \\ & X^{-1} & \\ & & X^{-1} \end{bmatrix} \begin{bmatrix} B & & \\ & B & \\ & & B \end{bmatrix} \begin{bmatrix} X & & \\ & X & \\ & & X \end{bmatrix} = \begin{bmatrix} \Lambda & & \\ & \Lambda & \\ & & \Lambda \end{bmatrix}$$

where

$$\Lambda = \begin{bmatrix} \lambda_1 & & & \\ & \lambda_2 & & \\ & & \lambda_3 & \\ & & & \lambda_4 \end{bmatrix}$$

Notice that the matrix  $A_y^{(x)}$  is *transparent* to this transformation. That is, if we set  $X \equiv \text{diag}(X)$

$$X^{-1} \begin{bmatrix} \tilde{b}_0 \cdot I & \tilde{b}_1 \cdot I & \\ \tilde{b}_{-1} \cdot I & \tilde{b}_0 \cdot I & \tilde{b}_1 \cdot I \\ & \tilde{b}_{-1} \cdot I & \tilde{b}_0 \cdot I \end{bmatrix} X = \begin{bmatrix} \tilde{b}_0 \cdot I & \tilde{b}_1 \cdot I & \\ \tilde{b}_{-1} \cdot I & \tilde{b}_0 \cdot I & \tilde{b}_1 \cdot I \\ & \tilde{b}_{-1} \cdot I & \tilde{b}_0 \cdot I \end{bmatrix}$$

One now permutes the transformed system to the y-vector data-base using the permutation matrix defined by Eq. 12.13. There results

$$P_{yx} \cdot X^{-1} [A_x^{(x)} + A_y^{(x)}] X \cdot P_{xy} =$$

$$\begin{bmatrix} \lambda_1 \cdot I & & & \\ & \lambda_2 \cdot I & & \\ & & \lambda_3 \cdot I & \\ & & & \lambda_4 \cdot I \end{bmatrix} + \begin{bmatrix} \tilde{B} & & & \\ & \tilde{B} & & \\ & & \tilde{B} & \\ & & & \tilde{B} \end{bmatrix}$$

where  $\tilde{B}$  is the banded tridiagonal matrix  $B(\tilde{b}_{-1}, \tilde{b}_0, \tilde{b}_1)$ , see the bottom of Eq. 12.23. Next find the eigenvectors  $\tilde{X}$  that diagonalize the  $\tilde{B}$  blocks. Let  $\tilde{\Lambda} \equiv \text{diag}(\tilde{B})$  and  $\tilde{X} \equiv \text{diag}(\tilde{X})$  and form the second transformation

$$\tilde{X}^{-1} \tilde{B} \tilde{X} = \begin{bmatrix} \tilde{\Lambda} & & & \\ & \tilde{\Lambda} & & \\ & & \tilde{\Lambda} & \\ & & & \tilde{\Lambda} \end{bmatrix}, \quad \tilde{\Lambda} = \begin{bmatrix} \tilde{\lambda}_1 & & \\ & \tilde{\lambda}_2 & \\ & & \tilde{\lambda}_3 \end{bmatrix}$$

This time, by the same argument as before, the first matrix on the right side of Eq. 13.13 is transparent to the transformation, so the final result is the complete diagonalization of the matrix  $A_{x+y}$

$$[\tilde{X}^{-1} \cdot P_{yx} \cdot X^{-1}] [A_{x+y}^{(x)}] [X \cdot P_{xy} \cdot \tilde{X}] = \begin{bmatrix} \lambda_1 I + \tilde{\Lambda} & & & \\ & \lambda_2 I + \tilde{\Lambda} & & \\ & & \lambda_3 I + \tilde{\Lambda} & \\ & & & \lambda_4 I + \tilde{\Lambda} \end{bmatrix}$$

It is important to notice that:

- The diagonal matrix on the right side of Eq. 13.13 contains every possible combination of the individual eigenvalues of  $B$  and  $\tilde{B}$ .

Now we are ready to present the representative equation for two dimensional systems. First reduce the PDE to ODE by some choice<sup>4</sup> of space differencing. This results in a spatially split  $A$  matrix formed from the subsets

$$A_x^{(x)} = \text{diag}(B) \quad , \quad A_y^{(y)} = \text{diag}(\tilde{B}) \quad (13.13)$$

where  $B$  and  $\tilde{B}$  are any two matrices that have linearly independent eigenvectors (this puts some constraints on the choice of differencing schemes).

Although  $A_x$  and  $A_y$  do commute, this fact, by itself, does not ensure the property of “all possible combinations”. To obtain the latter property the structure of

<sup>4</sup>We have used 3-point central differencing in our example, but this choice was for convenience only, and its use is not necessary to arrive at Eq. 13.13.

the matrices is important. The block matrices  $B$  and  $\tilde{B}$  can be either circulant or noncirculant; in both cases we are led to the final result:

The 2-D representative equation for model linear systems is

$$\frac{du}{dt} = [\lambda_x + \lambda_y]u + ae^{\mu t}$$

where  $\lambda_x$  and  $\lambda_y$  are *any combination* of eigenvalues from  $A_x$  and  $A_y$ ;  $a$  and  $\mu$  are (possibly complex) constants, and where  $A_x$  and  $A_y$  satisfy the conditions in 13.13.

Often we are interested in finding the value of, and the convergence rate to, the steady-state solution of the representative equation. In that case we set  $\mu = 0$  and use the simpler form

$$\frac{du}{dt} = [\lambda_x + \lambda_y]u + a \quad (13.14)$$

which has the exact solution

$$u(t) = ce^{(\lambda_x + \lambda_y)t} + \frac{a}{\lambda_x + \lambda_y} \quad (13.15)$$

## 13.5 Example Analysis of 2-D Model Equations

In the following we analyze four different methods for finding a fixed, steady-state solution to the 2-D representative equation 13.13. In each case we examine

1. The stability.
2. The accuracy of the fixed, steady-state solution.
3. The convergence rate to reach the steady-state.

### 13.5.1 The Unfactored Implicit Euler Method

Consider first this unfactored, first-order scheme which can then be used as a reference case for comparison with the various factored ones. The form of the method is given by Eq. 12.19, and when it is applied to the representative equation, we find

$$(1 - h\lambda_x - h\lambda_y)u_{n+1} = u_n + ha$$

from which

$$\begin{aligned} P(E) &= (1 - h\lambda_x - h\lambda_y)E - 1 \\ Q(E) &= h \end{aligned} \tag{13.16}$$

giving the solution

$$u_n = c \left[ \frac{1}{1 - h\lambda_x - h\lambda_y} \right]^n - \frac{a}{\lambda_x + \lambda_y}$$

Like its counterpart in the 1-D case, this method:

1. Is unconditionally stable.
2. Produces the exact (see Eq. 13.15) steady-state solution (of the ODE) for any  $h$ .
3. Converges very rapidly to the steady-state when  $h$  is large.

Unfortunately, however, use of this method for 2-D problems is generally impractical for reasons discussed in Section 12.5.

### 13.5.2 The Factored Nondelta Form of the Implicit Euler Method

Now apply the factored Euler method given by Eq. 12.20 to the 2-D representative equation. There results

$$(1 - h\lambda_x)(1 - h\lambda_y)u_{n+1} = u_n + ha$$

from which

$$\begin{aligned} P(E) &= (1 - h\lambda_x)(1 - h\lambda_y)E - 1 \\ Q(E) &= h \end{aligned} \tag{13.17}$$

giving the solution

$$u_n = c \left[ \frac{1}{(1 - h\lambda_x)(1 - h\lambda_y)} \right]^n - \frac{a}{\lambda_x + \lambda_y - h\lambda_x\lambda_y}$$

We see that this method:

1. Is unconditionally stable.

2. Produces a steady state solution that depends on the choice of  $h$ .
3. Converges rapidly to a steady-state for large  $h$ , but the converged solution would be completely wrong.

The method is easy to put on a computer and demands very little storage. However, it is not very useful since its transient solution is only first-order accurate and, if one tries to take advantage of its rapid convergence rate, the converged value is meaningless.

### 13.5.3 The Factored Delta Form of the Implicit Euler Method

Next apply Eq. 12.30 to the 2-D representative equation. One finds

$$(1 - h \lambda_x)(1 - h \lambda_y)(u_{n+1} - u_n) = h(\lambda_x u_n + \lambda_y u_n + a)$$

which reduces to

$$(1 - h \lambda_x)(1 - h \lambda_y)u_{n+1} = (1 + h^2 \lambda_x \lambda_y)u_n + ha$$

and this has the solution

$$u_n = c \left[ \frac{1 + h^2 \lambda_x \lambda_y}{(1 - h \lambda_x)(1 - h \lambda_y)} \right]^n - \frac{a}{\lambda_x + \lambda_y}$$

This method:

1. Is unconditionally stable.
2. Produces the exact steady-state solution for any choice of  $h$ .
3. Converges very slowly to the steady-state solution for large values of  $h$ , since  $|\sigma| \rightarrow 1$  as  $h \rightarrow \infty$ .

Like the factored nondelta form, this method is easy to put on a computer and demands very little storage. It is a basic option in the Ames research codes ARC2D and ARC3D, but many sophisticated numerical “tricks” have been incorporated to speed up its convergence to rate.

### 13.5.4 The Factored Delta Form of the Trapezoidal Method

Finally consider the delta form of a second-order time-accurate method. Apply Eq. 12.29 to the representative equation and one finds

$$\left(1 - \frac{1}{2}h\lambda_x\right)\left(1 - \frac{1}{2}h\lambda_y\right)(u_{n+1} - u_n) = h(\lambda_x u_n + \lambda_y u_n + a)$$

which reduces to

$$\left(1 - \frac{1}{2}h\lambda_x\right)\left(1 - \frac{1}{2}h\lambda_y\right)u_{n+1} = \left(1 + \frac{1}{2}h\lambda_x\right)\left(1 + \frac{1}{2}h\lambda_y\right)u_n + ha$$

and this has the solution

$$u_n = c \left[ \frac{\left(1 + \frac{1}{2}h\lambda_x\right)\left(1 + \frac{1}{2}h\lambda_y\right)}{\left(1 - \frac{1}{2}h\lambda_x\right)\left(1 - \frac{1}{2}h\lambda_y\right)} \right]^n - \frac{a}{\lambda_x + \lambda_y}$$

This method:

1. Is unconditionally stable.
2. Produces the exact steady-state solution for any choice of  $h$ .
3. Converges very slowly to the steady-state solution for large values of  $h$ , since  $|\sigma| \rightarrow 1$  as  $h \rightarrow \infty$ .

All of these properties are identical to those found for the factored delta form of the implicit Euler method. Furthermore, these two methods are equally easy to put on a computer<sup>5</sup> and they take exactly the same amount of storage. This method is also an option in the Ames research codes ARC2D and ARC3D. Since it is second order in time, it is usually used when time accuracy is desired, and the factored delta form of the implicit Euler method (with its attendant acceleration tricks) is usually used when a converged steady-state is all that is required. A brief inspection of eqs. 12.26 and 12.27 should be enough to convince the student that the  $\sigma$ 's produced by those methods are identical to the  $\sigma$  produced by this method.

## 13.6 Example Analysis of the 3-D Model Equation

The arguments in Section 13.4 generalize to three dimensions and, under the conditions given in 13.13 with an  $A_z^{(z)}$  included, the model 3-D cases<sup>6</sup> have the unforced

<sup>5</sup>In practical codes, the value of  $h$  on the left side of the implicit equation is literally switched from  $h$  to  $\frac{1}{2}h$ .

<sup>6</sup>Eqs. 13.11 and 13.12, each with an additional term.

representative equation

$$\frac{du}{dt} = [\lambda_x + \lambda_y + \lambda_z]u + a \quad (13.18)$$

Let us analyze a 2nd-order accurate, factored, delta form using this equation. First apply the trapezoidal method:

$$u_{n+1} = u_n + \frac{1}{2}h[(\lambda_x + \lambda_y + \lambda_z)u_{n+1} + (\lambda_x + \lambda_y + \lambda_z)u_n + 2a]$$

Rearrange terms:

$$\left[1 - \frac{1}{2}h(\lambda_x + \lambda_y + \lambda_z)\right]u_{n+1} = \left[1 + \frac{1}{2}h(\lambda_x + \lambda_y + \lambda_z)\right]u_n + ha$$

Put this in delta form:

$$\left[1 - \frac{1}{2}h(\lambda_x + \lambda_y + \lambda_z)\right]\Delta u_n = h[(\lambda_x + \lambda_y + \lambda_z)u_n + a]$$

Now factor the left side:

$$\left(1 - \frac{1}{2}h\lambda_x\right)\left(1 - \frac{1}{2}h\lambda_y\right)\left(1 - \frac{1}{2}h\lambda_z\right)\Delta u_n = h[(\lambda_x + \lambda_y + \lambda_z)u_n + a] \quad (13.19)$$

This preserves second order accuracy since the error terms

$$\frac{1}{4}h^2(\lambda_x\lambda_y + \lambda_x\lambda_z + \lambda_y\lambda_z)\Delta u_n \quad \text{and} \quad \frac{1}{8}h^3\lambda_x\lambda_y\lambda_z$$

are both  $O(h^3)$ . One can derive the characteristic polynomial for Eq. 13.19, find the  $\sigma$  root, and write the solution either in the form

$$u_n = c \left[ \frac{1 + \frac{1}{2}h(\lambda_x + \lambda_y + \lambda_z) + \frac{1}{4}h^2(\lambda_x\lambda_y + \lambda_x\lambda_z + \lambda_y\lambda_z) - \frac{1}{8}h^3\lambda_x\lambda_y\lambda_z}{1 - \frac{1}{2}h(\lambda_x + \lambda_y + \lambda_z) + \frac{1}{4}h^2(\lambda_x\lambda_y + \lambda_x\lambda_z + \lambda_y\lambda_z) - \frac{1}{8}h^3\lambda_x\lambda_y\lambda_z} \right]^n - \frac{a}{\lambda_x + \lambda_y + \lambda_z} \quad (13.20)$$

or in the form

$$u_n = c \left[ \frac{\left(1 + \frac{1}{2}h\lambda_x\right)\left(1 + \frac{1}{2}h\lambda_y\right)\left(1 + \frac{1}{2}h\lambda_z\right) - \frac{1}{4}h^3\lambda_x\lambda_y\lambda_z}{\left(1 - \frac{1}{2}h\lambda_x\right)\left(1 - \frac{1}{2}h\lambda_y\right)\left(1 - \frac{1}{2}h\lambda_z\right)} \right]^n - \frac{a}{\lambda_x + \lambda_y + \lambda_z} \quad (13.21)$$

It is interesting to notice that a Taylor series expansion of Eq. 13.21 results in

$$\begin{aligned} \sigma &= 1 + h(\lambda_x + \lambda_y + \lambda_z) + \frac{1}{2}h^2(\lambda_x + \lambda_y + \lambda_z)^2 \\ &+ \frac{1}{4}h^3[\lambda_z^3 + (2\lambda_y + 2\lambda_x) + (2\lambda_y^2 + 3\lambda_x\lambda_y + 2\lambda_y^2) + \lambda_y^3 + 2\lambda_x\lambda_y^2 + 2\lambda_x^2\lambda_y + \lambda_x^3] + \dots \end{aligned} \quad (13.22)$$

which verifies the second order accuracy of the factored form. Furthermore, clearly, if the method converges, it converges to the proper steady-state.<sup>7</sup>

With regards to stability, it follows from Eq. 13.20 that, if all the  $\lambda$ 's are real and negative, the method is stable for all  $h$ . This makes the method *unconditionally stable* for the 3-D *diffusion* model when it is centrally differenced in space.

Now consider what happens when we apply this method to the biconvection model, the 3-D form of Eq. 13.12 with periodic boundary conditions. In this case, central differencing causes all of the  $\lambda$ 's to be imaginary with spectrums that include both positive and negative values. *Remember that in our analysis we must consider every possible combination of these eigenvalues.* First write the  $\sigma$  root in Eq. 13.20 in the form

$$\sigma = \frac{1 + i\alpha - \beta + i\gamma}{1 - i\alpha - \beta + i\gamma}$$

where  $\alpha$ ,  $\beta$  and  $\gamma$  are real numbers that can have any sign. Now we can always find one combination of the  $\lambda$ 's for which  $\alpha$ , and  $\gamma$  are both positive. In that case since the absolute value of the product is the product of the absolute values

$$|\sigma|^2 = \frac{(1 - \beta)^2 + (\alpha + \gamma)^2}{(1 - \beta)^2 + (\alpha - \gamma)^2} > 1$$

and the method is *unconditionally unstable* for the model *convection* problem.

From the above analysis one would come to the conclusion that the method represented by Eq. 13.19 should not be used for the 3-D Euler equations. In practical cases, however, some form of dissipation is almost always added to methods that are used to solve the Euler equations and our experience to date is that, in the presence of this dissipation, the instability disclosed above is too weak to cause trouble. Consequently, the method is used as the basis for the Ames research code ARC3D.

---

<sup>7</sup>However, we already knew this because we chose the delta form.